CEP3: Community Event Prediction with Neural Point Process on Graph

Anonymous Author(s)
Anonymous Affiliation
Anonymous Email

Abstract

Many real world applications can be formulated as event forecasting on Continuous Time Dynamic Graphs (CTDGs) where the occurrence of a timed event between two entities is represented as an edge along with its occurrence timestamp. However, many previous works handle the problem in compromised settings, either formulating it as a link prediction task on the graph given the event time, or a time prediction problem for event will happen next. In this paper, we propose a novel model combining Graph Neural Networks and Marked Temporal Point Process (MTPP) that jointly forecasts multiple link events and their timestamps on communities over a CTDG. Moreover, to scale our model to large graphs, we factorize the jointly event prediction problem into three easier conditional probability modeling problems. To evaluate the effectiveness of our model and the rationale behind such a decomposition, we establish a set of benchmarks and evaluation metrics. The experimental results demonstrate the superiority of our model in terms of both accuracy and training efficiency. All the source codes and datasets are available at an anonymous repository and will be made publicly available.

1 Introduction

Modeling dynamic interactions of entities has become an important topic in different applications across many fields. In particular, studying the evolution of community social events can enable preemptive intervention for the pandemic (e.g., COVID-19) spreading [1]. Monitoring and forecasting the spreading of traffic congestion [2] can help to prevent congestion expanding to outside of the local area. The community needs more attention and help if there is a sudden change in the state of the economic [3] or political leanings [4]. In some cases, some entities, such as those with dense connections, or with similar characteristics, may form certain communities, and communities could also be defined by users based on their criteria. In reality, people may only be interested in a specific community of entities' interactions in some practical applications, such as community behavior modeling [5], dynamic community discovery [6] and community outliers detection [7].

Transformer Hawkes [8] is the first progress that incorporates the graph structure information into a temporal point process to jointly predict the incident nodes and timestamp. However, it only supports reasoning future events on the static graph with dynamic node properties, losing the flexibility to process structurally changing dynamic graphics. For better understanding and forecasting the events in a community, we suggest organizing event stream as a Continuous Time Dynamic Graphs (CTDG), and predicting a series of future events not only about **which** two entities will be involved but also **when** they will occur.

CTDG [9] is a common representation paradigm for organizing dynamic interaction event stream over time, with edges and nodes denoting the events with timestamp and the pairwise involved entities, respectively. Formally, denote a CTDG as $G = (V, E_T)$, where $E_T = \{\varepsilon_i : i = 1, \cdots, T\}$ is the set of edges, $\varepsilon_i = (u_i, v_i, t_i)$ with source node u_i, destination node v_i, and timestamp t_i. The edges are ordered by timestamps, i.e., $t_i \le t_j$ given $1 \le i \le j \le T$. We further denote a CTDG within a temporal window as $G_{i:j} = (V, E_{i:j})$ where $E_{i:j} = \{\varepsilon_k : i \le k < j\}$. Given the queried community (or node candidates that people are interested in) $C_q \subset V$, predicting K future events within the community given n observed events requires to model the following conditional distribution:

$$p(\varepsilon_{n+1}, \cdots, \varepsilon_{n+K} \mid G_{1:n}, C_q) \tag{1}$$

where the distribution of each edge ε_{n+i} is further a triple joint probability distribution of its source and destination nodes as well as its timestamp. Community event forecasting task is illustrated using Fig. 5 in Appendix A. Compared with traditional time series prediction, event forecasting on a CTDG jointly consider the spatial information characterized by the graph and the temporal signal characterized by the event stream to make a more accurate prediction.

There have been several lines of work to approach the problem but all in compromised settings. Temporal Graph Neural Networks (TGNNs) extends GNNs of static graphs to CTDGs by incorporating temporal signals into the message passing procedure. Most of TGNN progress [10–12] focuses on *temporal link prediction* task, i.e., modeling the conditional distribution $p(v_{n+1} \mid G_{1:n}, u_{n+1}, t_{n+1})$. Other parts of the progress uses Temporal Point Process (TPP) for *event timestamp prediction* which predicts the time of the next event but requires the entities to be known, i.e., modeling the conditional distribution $p(t_{n+1} \mid G_{1:n}, u_{n+1}, v_{n+1})$. All these models are not directly applicable to the event forecasting problem on CTDGs.

Marked TPP (MTPP) and its variations such as Recurrent Marked Temporal Point Process (RMTPP) [13] associate each event with a marker and jointly predict the marker as well as the timestamp of future events. MTPP and RMTPP are capable of predicting CTDG events by treating the entity pair (u_i, v_i) as the event marker. However, these kinds of MTPP-based methods face three major drawbacks. To begin with, MTPP methods treat edges as individual makers, which are unable to utilize the community and relationship information, resulting in a suboptimal training solution. Besides, individual makers also bring an $O(|V|^2)$ marker distribution space, making the model less scalable to large graphs. The last difficulty is that RMTPP is further constrained by its recurrent structure, which must process each event sequentially for keeping events' contextual correlation.

Our contributions in this paper are:

i) We handle the **C**ommunity **E**vent **P**redicting task with a graph **P**oint **P**rocess model (**CEP3**), which is significantly harder than both standalone temporal link prediction and timestamp prediction tasks. Our model incorporates both spatial and temporal signals using GNNs and TPPs and can predict event entities and timestamps simultaneously.

ii) To scale to large graphs, we factorize the mark distribution of MTPP and reduce the computational complexity from $O(|V|^2)$ of previous TPP attempts [13, 14] to $O(|V|)$. Moreover, we employ a time-aware attention model to replace the TPP model's recurrent structure, significantly shortening the sequence length of each training step and enabling mini-batches training.

iii) We propose new benchmarks for the community event forecasting task on a CTDG. Specifically, we design new evaluation metrics measuring prediction quality of both entities and timestamps. For baselines, we collect and carefully adapt state-of-the-art models from time series prediction, temporal link prediction and timestamp prediction. Our evaluation shows that CEP3 is superior across all four real-world graph datasets. Source code has been already made publicly available.

2 Related Work Analysis

2.1 Temporal Graph Learning

Temporal Graph Learning aims at learning node embeddings using both structural and temporal signals, which gives rise to a number of works. CTDNE [15] and CAWs [9] incorporate temporal random walks into skip-gram model for capturing temporal motif information in CTDGs. JODIE [10] and TigeCMN [16] adopt recurrent neural networks (RNNs) and attention-based memory module respectively to update node embedding dynamically. Temporal Graph Neural Networks like TGAT [12] and TGN [11] enhance the attention-based message passing process from Graph Neural Networks with Fourier time encoding kernel. These attempts focus on the temporal link prediction task. Besides that, other works [17, 18] focus on information diffusion task which aims at predicting whether a user will perform an action at time t. None of them is designed for event forecasting.

RE-Net [19] and CoNN [5] study a similar event forecasting setting on Discrete Temporal Dynamic Graphs (DTDGs). However, continuous time prediction is much harder and their methods cannot be directly applied.

2.2 Neural Temporal Point Process

A temporal point process (TPP) [20] is a stochastic process modeling the distribution of a sequence of events associated with continuous timestamps $t_1, \cdots, t_n$. The theoretical underpinnings and wide-ranging practical applications of the TPP methods are described in Appendix B. The majority of neural TPP approaches leverage recurrent neural network (RNN)[13, 21–23] based structure to parametrize the stochastic process function and forecast the future events. Such approach cannot be trained in parallel and cannot capture long-term dependencies. Transformer Hawkes [8] replace RNN module with temporal aware attention transformer to capture temporal dependencies.

However, these methods cannot be directly applied to event forecasting on CTDGs due to the following reasons. First, a CTDG is essentially a *single* event sequence, whose length ranges from tens of thousands to hundreds of millions. RNNs (even LSTMs) are known to have trouble dealing with very long sequences. One may consider dividing the sequence into multiple shorter windows, which will make the events disconnected within the given window and discard all the data before it. This fails to explore the dependencies between events that are distant over time but topologically connected (i.e. sharing either of the incident nodes). One may also consider training an RMTPP with Truncated BPTT [24] on the long sequence as a whole. However, this is inefficient because parallel training is impossible due to its recurrent nature, which means that one has to unroll the sequence one event at a time. Second, although Transformer Hawkes [8] discards the RNN structure, it directly models the marker generation distribution with a unit softmax function will produce a vector with space complexity of $O(|V|^2)$, as the event markers will be essentially the events' incident node pairs. This is not applicable to dynamic graphs with changing structure and undesirable for large graphs.

2.3 Temporal Point Process on Dynamic Graph

Previous works, such as [14, 25–27], use kinds of recurrent architecture to approximate temporal point process over graphs. However, recurrent architecture prevents the model from parallelized minibatch training, which is undesirable especially on large-scale graphs. This is because learning long-term dependencies using recurrent architecture requires the model to traverse the event sequence one by one instead of randomly mini-batch selection.

MMDNE [28], HTNE [29] and DSPP [30] employ the attention mechanism to avoid the inefficiency of the recurrent structure in training with large CTDGs. However, these works are restrictively dedicated to link prediction or timestamp prediction task. Adapting the two models to event forecasting requires non-trivial changes since neither of them handles efficient joint forecasting of the event's incident nodes.

3 Model

Our model is depicted in Fig. 1. To predict the next K events $\varepsilon_{n+1}, \cdots, \varepsilon_{n+K}$ given the history graph $G_{1:n}$, we first obtain an initial representation $\mathbf{h}^{(0)}$ for every node using an GNN Encoder, as well as an initial graph $\tilde{G}^{(0)}$. Then for the i-th step, we predict $\varepsilon_{n+i} = (u_{n+i}, v_{n+i}, t_{n+i})$, i.e. the source node, destination node, and timestamp for the next i-th event. The predicted event is then added into $\tilde{G}^{(i-1)}$ to form $\tilde{G}^{(i)}$, to keep track of what we have predicted so far. The hidden states $\mathbf{h}^{(i)}$ are then updated from the new graph $\tilde{G}^{(i)}$ and $\mathbf{h}^{(i-1)}$. This generally follows the framework of RMTPP [13], except that **i)** we initialize the beginning states of **Auto-Regressive Message Passing** Module with a time-aware GNN, which allows our recurrent module to traverse over a much shorter sequence without losing historical information; **ii)** we update the **Auto-Regressive Message Passing** network states with a GNN to model the topological dependencies between entities caused by new events; and **iii)** we forecast the nodes and the timestamp for an event by decomposing the joint probability distribution. We give specific details of each component as follows.

3.1 Structural and Temporal GNN Encoder

The Encoder GNN Layer should be capable of encoding relational dependencies, timestamps, and optionally edge features at the same time. The encoded node representations is used by the forecaster in next section to generate the predicted events. It has the following form:

$$\mathbf{z}_v^{(l)} = f_{\text{agg}}^{\text{enc}}(\mathbf{z}_v^{(l-1)}, \{g_{\text{msg}}^{\text{enc}}(\mathbf{z}_u^{(l-1)}, \mathbf{e}_{uv}^t, \phi(t_n - t)) : (u, t, \mathbf{e}_{uv}^t) \in \mathcal{N}^v\}) \quad (2)$$

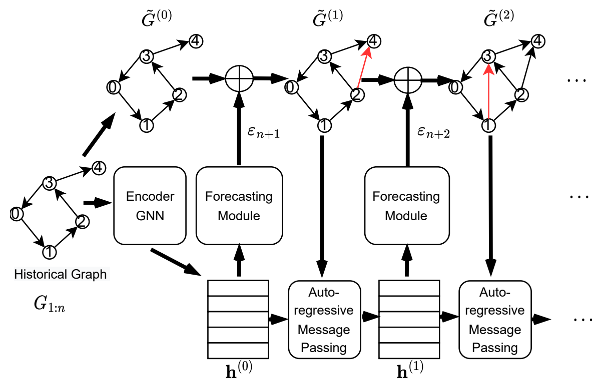

Figure 1: The overall architecture of proposed CEP3 model. Red arrows represent the predicted events ε_{n+i}.

where $\mathcal{N}^v$ is the brief formulation of $\mathcal{N}^v[1:n]$, which represents the subgraph induced by the 1-hop neighborhood of node i on the graph $G_{1:n}$, and $\phi(t)$ are learnable time encodings used in [11, 12, 31]. $f_{\text{agg}}^{\text{enc}}$ and $g_{\text{msg}}^{\text{enc}}$ can be any aggregation and message functions of a GNN-based representation encoder. $\mathbf{z}_v^{(0)}$ could be either node v's feature vector, and $\mathbf{e}_{uv}^t$ means the edge feature between node u and v at time t.

We use a GNN to initialize the recurrent network's states because it takes the historical events within a topological local neighborhood, including the incident nodes, the timestamps, and the feature of events together as input, while enabling us to train on multiple history graphs in parallel. In particular, we use a neighborhood graph temporal attention based method for encoding, whose detailed formulation is as follows. Temporal Graph Attention Module is a self attention based node embedding method inspired by [12], the detailed formulation is as below:

$$\begin{aligned}
\mathbf{z}_v^{(l)} &= \texttt{MLP}(\mathbf{z}_v^{(l-1)}||\tilde{\mathbf{z}}_v^{(l)}) \\
\tilde{\mathbf{z}}_v^{(l)} &= \texttt{MultiHeadAttn}^{(l)}(\mathbf{q}_v^{(l)}, \mathbf{K}_v^{(l)}, \mathbf{V}_v^{(l)}) \\
\mathbf{q}_v^{(l)} &= [\mathbf{z}_v^{(l-1)}||\phi(0)] \\
\mathbf{K}_v^{(l)} &= \mathbf{V}_v^{(l)} = \mathbf{C}_v^{(l)} \\
\mathbf{C}_v^{(l)} &= [\mathbf{z}_u^{(l-1)}||\mathbf{e}_{uv}^{t_u}||\phi(t_v - t_u), u \in \mathcal{N}^v]
\end{aligned} \tag{3}$$

The multi-head attention is computed as:

$$\tilde{\mathbf{z}}_v^{(l)} = \sum_{a}^{\forall head} \text{SoftMax}\left(\frac{(\mathbf{W}_{Q,a}^{(l)}\mathbf{q}_v^{(l)})(\mathbf{W}_{K,a}^{(l)}\mathbf{K}_v^{(l)})}{\sqrt{d_q}}\right)\left(\mathbf{W}_{V,a}^{(l)}\mathbf{V}_v^{(l)}\right) \tag{4}$$

where $\mathbf{W}_{Q,a}^{(l)}$ means one head of multi-head attention weight matrix and d_q means the dimension of the vector $\mathbf{q}_v^{(l)}$. The temporal encoding module is the same as in [11, 12] original paper:

$$\phi(\Delta t) = \frac{1}{\sqrt{d_w}}\cos(\vec{\mathbf{w}}\Delta t + \vec{\mathbf{b}}) \tag{5}$$

where $\vec{\mathbf{w}}$ and $\vec{\mathbf{b}}$ are learnable parameters, d_w is the dimension of weight vector $\mathbf{w}$.

Although a GNN cannot consider events outside the neighborhood, we argue that the impact is minimal. We empirically verify this argument by comparing against the variant that uses both attention and RNN based memory module in the training phase (named **CEP3 w RNN**), which can incorporate historical events and time-aware information by the view of topological locality and recursive impact, respectively. However, RNN takes drastically more memory and time in training because of the same reason in Section 2.3.

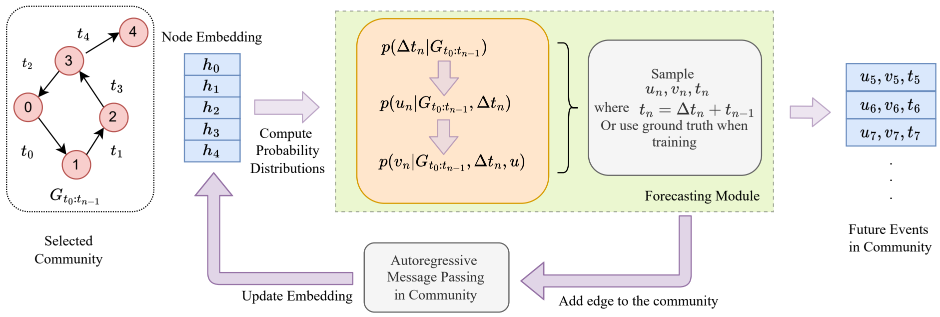

Figure 2: The hierarchical probability-chain forecaster and its workflow relationship with the auto-regressive message passing module. The node embeddings are learned from the GNN Encoder described in Section 3.1. Note that the 'selected community' refers to an application-dependent collection of candidate nodes for query.

3.2 Hierarchical Probability-Chain Forecaster

Fig. 2 demonstrates the details of our event forecaster. We can see that the forecaster predicts future events only according to node embeddings and historical connections in the selected candidates (or communities). It means that we do not have to be concerned about a large number of communities which are likely to slow down the process, because CEP3 model can handle numerous communities simultaneously during training and inference.

From the superposition property [32] of an MTPP described in Section 2.2, we forecast the next event $\varepsilon_{n+i} = (u_{n+i}, v_{n+i}, t_{n+i})$ by a triple probability-chain:

$$p(u_{n+i}, v_{n+i}, t_{n+i}) = p(t_{n+i})p(u_{n+i} \mid t_{n+i})p(v_{n+i} \mid t_{n+i}, u_{n+i}) \tag{6}$$

It means that we can predict first the timestamp, then the source node, and finally the destination node. We predict t_{n+i} by modeling the distribution of the time difference as follows:

$$\begin{aligned} \eta_v^{(i)} &= \mathrm{Softplus}(\mathrm{MLP_t}(\mathbf{h}_v^{(i-1)})) \\ \lambda_i &= \sum_{v \in V} \eta_v^{(i)} \\ \Delta t_{n+i} &\sim Exponential(\lambda_i) \\ t_{n+i} &= t_n + \Delta t_{n+i} \end{aligned} \tag{7}$$

where the $\mathbf{h}_v^{(0)}$ is initialized using the node representation learned by $\mathbf{z}_v^{(L)}$, and $\mathrm{Softplus}$ ensures that $\eta_v^{(i)}$ is above zero and the gradient still exists for negative $\eta_v^{(i)}$ values. MLP_t represents a multilayer perceptron to generate the intensity value of time. Since Δt_{n+i} obeys exponential distribution, we simply sample the mean value of time intensity distribution, $\frac{1}{\lambda_i}$, as the final Δt_{n+i} output during training. The conditional intensity of the next event occurring on *one* of the nodes in V is thus the sum of all $\eta_v^{(i)}$ [32]. Other conditional intensity choices are also possible.

We then generate the source node u_{n+i} of event ε_{n+i} from a categorical distribution conditioned on t_{n+i}, parameterized by another MLP:

$$p(u_{n+i} \mid t_{n+i}) = \mathrm{Softmax}(\mathrm{MLP_{src}}(\mathbf{h}_u^{(i-1)} \| \phi(\Delta t_{n+i}))) \tag{8}$$

where $\|$ means the concatenation operation and ϕ has the same form as in Eq. 2. We then generate the destination node v_{n+i} similarly, conditioned on t_{n+i} and u_{n+i}:

$$p(v_{n+i} \mid t_{n+i}, u_{n+i}) = \mathrm{Softmax}(\mathrm{MLP_{dst}}(\mathbf{h}_v^{(i-1)} \| \mathbf{h}_{u_{n+i}}^{(i-1)} \| \phi(\Delta t_{n+i}))) \tag{9}$$

Note that the formulation above will only generate two distributions that have $|V|$ elements, instead of $|V|^2$ as in RMTPP[13]. The implication is that during inference the strategy will be *greedy*: we first pick whatever source node that has the largest probability, then we pick the destination node conditioned on the picked source node. To verify the impact of this design choice, we also explore a variant of our method where we generate a joint distribution of the pair (u_{n+i}, v_{n+i}) with $O(|V|^2)$ elements, which we name **CEP3 w/o HRCHY** (short for Hierarchy). Hierarchy is the noun form of the word 'hierarchical'.

The proposed **CEP3** model obeys the probabilistic form of Eq. 6, while the ablation model **CEP3 w/o HRCHY** decomposes $p(u_{n+i}, v_{n+i}, t_{n+i})$ into $p(t_{n+i}) \times p(u_{n+i}, v_{n+i} \mid t_{n+i})$. If a graph has a lot of nodes, evaluating $p(u_{n+i}, v_{n+i})$ will incur a linear projection with $O(|V|^2)$ complexity. This is another obstacle to scaling up to larger datasets.

3.3 Auto-Regressive Message Passing

As shown in Fig. 2, we assume that an event's occurrence will directly influence the hidden states of its incident nodes. Moreover, the influence will propagate to other nodes along the links created by historical interactions. Therefore, after generating the new event ε_{n+i}, we would like to update the nodes' hidden states by message passing on the graph with the new events. We achieve that by maintaining another graph $\tilde{G}^{(i)}$ that keeps track of the graph with the historical interactions $G_{1:n}$ and the newly predicted events up to ε_{n+i}.

Specifically, we initialize $\tilde{G}^{(0)}$ with the candidate node set C as its nodes. The resulting graph encompasses the dependency between candidate nodes during the encoding stage. Every time a new event ε_{n+i} is predicted, we add the event back in: $\tilde{G}^{(i)} = \tilde{G}^{(i-1)} \cup \varepsilon_{n+i}$.

Afterwards, we update the nodes' hidden states using a message passing network such as GCN [33] for spatial propagation and a GRU [34] for temporal propagation:

$$\begin{aligned}
\mathbf{w}_v^{(i,0)} &= \mathbf{h}_v^{(i-1)} \\
\mathbf{w}_v^{(i,l)} &= f_{\text{agg}}^{\text{upd}}(\{g_{\text{msg}}^{\text{upd}}(\mathbf{w}_u^{(i,l-1)}, \mathbf{w}_v^{(i,l-1)}) : u \in \mathcal{N}_{\tilde{G}^{(i)}}^{v}\}) \\
\mathbf{h}_v^{(i)} &= \text{GRU}(\left[\mathbf{w}_v^{(i,L)} \| \phi(\Delta t_{n+1})\right], \mathbf{h}_v^{(i-1)})
\end{aligned} \tag{10}$$

where $\mathcal{N}_{\tilde{G}^{(i)}}^{v}$ is the neighboring events of node v in $\tilde{G}^{(i)}$, $f_{\text{agg}}^{\text{upd}}$ can be any message aggregation function and $g_{\text{msg}}^{\text{upd}}$ can be any message function.

To verify the necessity of updating the community using message passing after a event, we also explore a variant where we do not update all the node's hidden states in the community, but only the incident nodes u_{n+i} and v_{n+i}. We name this variant **CEP3 w/o AR**.

3.4 Loss Function and Prediction

The forecasting module outputs the next event's timestamp t_{n+i} and indicent nodes u_{n+i} and v_{n+i} for all events ε_{n+i}, which are minimized via negative log likelihood. Specifically, the loss function goes as follows:

$$\mathcal{L}_{\text{time}} = \sum_{i=1}^{K} [\underbrace{-\log(\lambda_i) + \Delta t_{n+i}\lambda_i}_{\text{time loss}} \underbrace{-\log p(u_{n+i}) - \log p(v_{n+i})}_{\text{entity loss}}] \tag{11}$$

where the first two terms within summation are log survival probability from Eq. 14 and the last two terms are log probabilities for source and destination node prediction. The time integration term $\int_{t_n}^{t} \lambda(\tau) d\tau$ in Eq. 14 is approximated using a first order integration method by $\lambda(t)\Delta t$ for the ease of computation.

4 Experiments

In this section, we test the performance and efficiency of the proposed methods against several baselines on four public real-world temporal graph datasets: Wikipedia, MOOC [10], GitHub [14], and SocialEvo [35]. The detailed description about datasets is put in the Appendix C. To verify the effectiveness of our CEP3 model, we suggested three ablation models (CEP3 w RNN, CEP3 w/o HRCHY. and CEP3 w/o AR) and five advanced methods (GRU, Hawkes Process [36], Poisson Process, RMTPP [13] and Dyrep [14]) as our baseline approach. Almost all baseline methods have been briefly explained in section 2 and 3. In Appendix D we explain why we choose these baselines and provide implementation details for better reproducibility. We also provide the details of our network architecture and the hyper-parameters in Appendix E. The source code is based on PyTorch and Deep Graph Library [37], which is anonymously available at `https://anonymous.4open.science/r/CEP-2567/`.

4.1 Evaluation Metrics

For evaluation on a specific dataset, we utilize the communities segmented by the conventional community detection algorithm Louvain [38] as the candidate node set, and we report the average result of all communities.

For each community C_q, we measure the perplexity (PP_{C_q}) of the ground truth source and destination node sequence for evaluating the node predicting performance, and evaluate the mean absolute error (MAE_{C_q}) of the predicted timestamps. Using our MAE to evaluate the quality of auto-regressive forecasting sequence over multiple timesteps can also be seen in traffic flow prediction [2].

Perplexity (PP) [39] is a concept in information theory that assesses how closely a probability model's projected outcome matches the real sample distribution. The less perplexity the situation, the higher the model's prediction confidence. In the field of natural language processing, perplexity is also commonly used to evaluate a language model's quality, i.e., to evaluate how closely the sentences generated by the language model match real human language samples. A language model predicts the next word from the word dictionary, whereas our event predicting model selects nodes from the node candidates (community). Therefore, it is reasonable to employ perplexity as a metric in our task.

Specifically, suppose we have the communities' ground truth event sequence (u_i, v_i, t_i) and the prediction sequence $(\hat{u}_i, \hat{v}_i, \hat{t}_i)$ where $i = 1, \cdots, K$. For we compute per step PP as

$$PP = \exp\left(-\frac{1}{K}\sum_{i=1}^{K}\left[\log p(u_i) + \log p(v_i \mid u_i)\right]\right) \tag{12}$$

For the distance between two sequences with difference lengths, we compute MAE [40]:

$$MAE = \frac{1}{K(t_K - t_0)}\sum_{i=1}^{K}\left[\left|t_i - \min(t_K, \hat{t}_i)\right|\right] \tag{13}$$

To keep it comparable in diverse datasets, the MAE is divided by the max time span $t_K - t_0$ and the sequence length K. We report the average PP_{C_q} of all communities as the PP of a certain dataset, and MAE is calculated in the same way. Smaller values of both metrics indicate better performance.

4.2 Result Analysis

From Table 1 we can see the notable superiority of CEP3 over other baselines in different datasets under both MAE and perplexity. The MAE difference between GRU and RMTPP show the effectiveness of temporal point process in predicting timestamps. Comparing CEP3 with sequence based TPP models RMTPP, we can see that using GNN to capture historical interaction information can improve the forecasting performance. Further more, when comparing **DyRep w AR** versus **DyRep** and **CEP3 w/o AR** versus pure **CEP3**, we can conclude that auto-regressive updates can better capture the impact of newly predicted events.

Our model performs better than DyRep w AR because in our CEP3, during the auto-regressive update, the newly predicted event not only influences the node involved in the event but also propagates to other nodes via message passing. It is worth mentioning that our CEP3 model is not only more effective than other baseline models in terms of performance, but it also allows parallel training and have faster training speed especially in large datasets. The training loss curve and analysis with different parallel sizes is shown in Appendix F.

4.3 Forecasting Visualization

From top to bottom, Fig. 3 visualizes the circle layout of a certain community within the graphs of the Github, Wikipedia and MOOC datasets, respectively. We plot the ground truth, our model's prediction and DyRep's prediction for comparison. The visualized graphs are generated as follows:

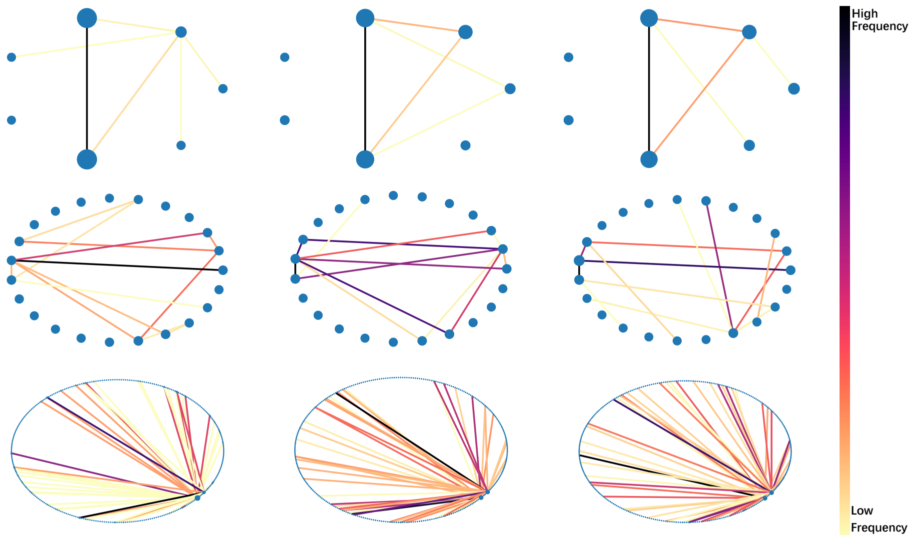

(a) Ground Truth. (b) CEP3. (c) DyRep.

Figure 3: Prediction visualizations of certain communities in the whole timespan of the test phase. The sizes of plotted nodes indicate their degrees, whereas the colors of edges represent the connection frequencies. Note that the edge colors and node sizes need be compared in the same row. The communities are from Github, Wikipedia and MOOC datasets, respectively, from top to bottom.

Table 1: Comparison of the average and standard deviation of perplexity of incident node prediction and mean absolute error of time prediction. The smaller the MAE and Perplexity, the better the model. The best result is highlighted in **bold** and second best is highlighted with underline. The Rank column shows the average ranking in each metric and dataset (the lower, the better).

Datasets	Wikipedia		Github		MOOC		SocialEvo		Rank
Metric	Perplexity	MAE	Perplexity	MAE	Perplexity	MAE	Perplexity	MAE	
GRU+Gaussian	131.06 ± 11.27	54.54 ± 1.19	68.53 ± 1.18	59.05 ± 1.72	457.40 ± 6.25	36.49 ± 2.01	33.85 ± 0.27	131.71 ± 7.09	8.00
Hawkes	108.00 ± 3.73	56.84 ± 0.31	74.40 ± 2.47	55.21 ± 0.12	502.31 ± 12.30	36.67 ± 0.29	45.33 ± 5.35	139.35 ± 0.17	9.50
Poisson	119.19 ± 1.11	56.70 ± 0.11	61.49 ± 0.96	55.21 ± 0.31	438.61 ± 7.05	36.61 ± 0.78	40.48 ± 1.99	139.3 ± 1.15	8.25
RMTPP w HRCHY	133.68 ± 2.31	34.15 ± 0.89	62.19 ± 0.88	55.05 ± 1.02	616.79 ± 25.74	32.29 ± 1.59	41.37 ± 6.55	140.02 ± 2.06	8.88
RMTPP	121.67 ± 1.01	32.91 ± 1.90	67.97 ± 1.02	54.79 ± 0.47	664.07 ± 11.05	32.83 ± 2.40	37.05 ± 0.77	138.9 ± 2.30	8.00
DyRep w AR	116.07 ± 4.98	28.74 ± 0.37	54.57 ± 1.82	28.46 ± 0.65	431.18 ± 1.18	29.92 ± 1.48	29.6 ± 1.93	99.96 ± 6.18	3.38
DyRep	119.13 ± 1.02	30.04 ± 0.14	64.05 ± 0.78	36.97 ± 1.74	438.61 ± 9.28	**13.41 ± 1.42**	36.59 ± 3.02	103.01 ± 3.49	4.75
CEP3 w RNN	104.87 ± 8.70	41.94 ± 1.89	60.18 ± 1.04	39.22 ± 2.93	374.77 ± 24.59	20.09 ± 0.33	30.37 ± 4.56	95.12 ± 2.25	3.88
CEP3 w/o HRCHY	**98.98 ± 7.61**	**28.69 ± 0.70**	52.04 ± 3.33	**26.8 ± 0.89**	**365.68 ± 28.01**	31.87 ± 0.18	**28.66 ± 2.74**	**79.58 ± 5.39**	**1.75**
CEP3 w/o AR	125.51 ± 7.64	39.31 ± 2.59	61.03 ± 1.03	34.03 ± 0.37	448.37 ± 4.34	21.4 ± 0.47	38.59 ± 1.02	95.21 ± 4.44	6.13
CEP3	118.82 ± 4.30	32.41 ± 0.58	**50.42 ± 0.70**	30.93 ± 1.67	401.64 ± 7.06	17.69 ± 2.68	36.8 ± 1.00	94.54 ± 7.31	3.25

We first apply the learned forecasting model to predict the edges using Monte Carlo sampling. This generation process is repeated for three times. We then discard generated edges that are not within the 33% highest prediction probabilities and obtain the final generated graph. Generating multiple times and then discarding the less possible edges is to reduce uncertainty in each one-time generated graphs.

In the first row, both CEP3 and DyRep capture the triangle connection in this small community. However, the triangle is lighter in the ground truth, which means that DyRep over-reinforces this connection in its predictions. In the second row, the prediction result of CEP3 is more similar to the truth, whereas DyRep generates a high-frequency purple edge which does not exist in the original graph. In the third row, CEP3 successfully learns the two black edges in ground truth, but DyRep predicts more than two links in darker colors.

We can see that our method successfully recognises the high-degree nodes capture many patterns of interactions as well as the evolution dynamics of the interactions graph, which includes the nodes with higher degrees. One pressing goal of community event prediction, rather than focusing on a single local node, is to anticipate if a certain high-frequency pattern will emerge in the community from a

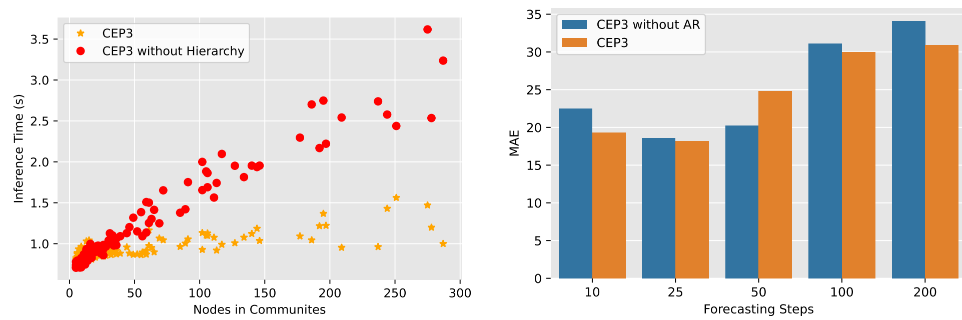

(a) Efficiency (b) Forecasting Steps

Figure 4: (a) To demonstrate the efficiency of proposed CEP3 hierarchical probability chain, we show 1000 steps' inference time cost against the node scale. In this scatter figure, each data point represents a community in the Wikipedia dataset (b) The number of forecasting step is an important parameter in almost all forecasting models. To further investigate the effect of the number of forecasting steps and the AR module on the CEP3 model, we run experiments with different numbers of forecasting steps. The small MAE, the better the model.

global perspective. Typical application cases include money laundering patterns [41] in finance and disease transmission patterns [42], etc.

4.4 Ablation Study

In Section 3 we have mentioned three variants: **CEP3 w RNN** to trade parallelized training for long-term dependency modeling with RNN based memory module, **CEP3 w/o HRCHY** to compare hierarchical (HRCHY) prediction versus joint prediction of incident nodes, and **CEP3 w/o AR** to compare using auto-regressive module versus not using.

CEP3 w/o HRCHY. The formulation without hierarchy structure yields a slower training and inference speed as shown in Fig. 4(a). We demonstrate that CEP3 is more efficient on large communities compared to CEP3 w/o HRCHY. As is shown in Fig. 4(a), computing intensity function of each possible node pair would take more time by orders of magnitude. We relax this issue by decomposing the node pair prediction problem into two node prediction sub-problems, which can be solved quicker especially in large scale communities.

CEP3 w/o AR. The model performance dropped significantly and yielded similar result as DyRep w AR. From Fig. 4(b), we can see that the AR forecasting is not always useful in all varying numbers of prediction steps. When the number of "prediction steps" is small (such as 10), CEP3 could just use the node embeddings at time t_n to predict the events. When the number of steps becomes larger, the systematic accumulated errors from AR gradually accumulate, leading to low MAE accuracy. And as the number of steps increases, the initial node embedding would have little effect in distant future events. This indicates that without AR, it may be difficult for the CEP3 model to accurately predict long-term occurrences.

CEP3 w RNN. The results show that the memory module brings performance improvement over pure CEP3, except on the Github dataset. The reason is perhaps that the Github dataset is a small one with a limited number of nodes and edges, and meanwhile it has a significantly longer timespan than other datasets. It means that the interaction is low-frequency in this situation, causing the insufficient memory updating.

5 Conclusion And Future Work

In this paper, we have formulated the community event forecasting task on a continuous time dynamic graph and set up benchmarks using the adaptation of the previous work. We further propose a new model to tackle this problem utilizing graph structures. We also address the scalability problem when formulating the temporal point process on the graph and reduce complexity with a hierarchical formulation. Experimental results show the prediction accuracy and training efficiency of our models.

However, this work remains two important limitations to solve. One is that we did not provide an experimental evaluation metric of the joint predictions because there are no widely accepted metrics that can be used directly now. We are already considering some metrics from the dynamic graph generation field [43] in future work. The other is that the evaluation is very dependent on the pre-defined communities detected by Louvain algorithm. Future work will contain comparisons utilizing different community detection algorithms (e.g. linkage algorithms [44], spectral clustering [45]).

References

[1] J Zhang and K Nawata. Multi-step prediction for influenza outbreak by an adjusted long short-term memory. *Epidemiology & Infection*, 146(7):809–816, 2018. 1

[2] Yaguang Li, Rose Yu, Cyrus Shahabi, and Yan Liu. Diffusion convolutional recurrent neural network: Data-driven traffic forecasting. In *International Conference on Learning Representations*, 2018. 1, 7

[3] Carlos Capistrán, Christian Constandse, and Manuel Ramos-Francia. Multi-horizon inflation forecasts using disaggregated data. *Economic Modelling*, 27(3):666–677, 2010. 1

[4] Stepan S Sulakshin. A quantitative political spectrum and forecasting of social evolution. *International Journal of Interdisciplinary Social Sciences*, 5(4), 2010. 1

[5] Yupeng Gu, Yizhou Sun, and Jianxi Gao. The co-evolution model for social network evolving and opinion migration. In *KDD*, pages 175–184. ACM, 2017. 1, 2

[6] Giulio Rossetti and Rémy Cazabet. Community discovery in dynamic networks: A survey. *ACM Comput. Surv.*, 51(2):35:1–35:37, 2018. 1

[7] Jing Gao, Feng Liang, Wei Fan, Chi Wang, Yizhou Sun, and Jiawei Han. On community outliers and their efficient detection in information networks. In *KDD*, pages 813–822. ACM, 2010. 1

[8] Simiao Zuo, Haoming Jiang, Zichong Li, Tuo Zhao, and Hongyuan Zha. Transformer hawkes process. In *ICML*, volume 119 of *Proceedings of Machine Learning Research*, pages 11692–11702. PMLR, 2020. 1, 3

[9] Yanbang Wang, Yen-Yu Chang, Yunyu Liu, Jure Leskovec, and Pan Li. Inductive representation learning in temporal networks via causal anonymous walks. In *International Conference on Learning Representations*, 2021. 1, 2

[10] Srijan Kumar, Xikun Zhang, and Jure Leskovec. Predicting dynamic embedding trajectory in temporal interaction networks. In *KDD*, pages 1269–1278. ACM, 2019. 2, 6, 14, 15

[11] Emanuele Rossi, Ben Chamberlain, Fabrizio Frasca, Davide Eynard, Federico Monti, and Michael M. Bronstein. Temporal graph networks for deep learning on dynamic graphs. *CoRR*, abs/2006.10637, 2020. 2, 4

[12] Da Xu, Chuanwei Ruan, Evren Körpeoglu, Sushant Kumar, and Kannan Achan. Inductive representation learning on temporal graphs. In *ICLR*. OpenReview.net, 2020. 2, 4

[13] Nan Du, Hanjun Dai, Rakshit Trivedi, Utkarsh Upadhyay, Manuel Gomez-Rodriguez, and Le Song. Recurrent marked temporal point processes: Embedding event history to vector. In *Proceedings of the 22nd ACM SIGKDD International Conference on Knowledge Discovery and Data Mining*, pages 1555–1564, 2016. 2, 3, 5, 6, 14, 16

[14] Rakshit Trivedi, Mehrdad Farajtabar, Prasenjeet Biswal, and Hongyuan Zha. Dyrep: Learning representations over dynamic graphs. In *ICLR (Poster)*. OpenReview.net, 2019. 2, 3, 6, 14, 15, 16

[15] Giang Hoang Nguyen, John Boaz Lee, Ryan A Rossi, Nesreen K Ahmed, Eunyee Koh, and Sungchul Kim. Continuous-time dynamic network embeddings. In *Companion Proceedings of the The Web Conference 2018*, pages 969–976, 2018. 2

[16] Zhen Zhang, Jiajun Bu, Martin Ester, Jianfeng Zhang, Chengwei Yao, Zhao Li, and Can Wang. Learning temporal interaction graph embedding via coupled memory networks. In *WWW*, pages 3049–3055. ACM / IW3C2, 2020. 2

[17] Dong Li, Shengping Zhang, Xin Sun, Huiyu Zhou, Sheng Li, and Xuelong Li. Modeling information diffusion over social networks for temporal dynamic prediction. *IEEE Trans. Knowl. Data Eng.*, 29(9):1985–1997, 2017. 2

[18] Qitian Wu, Yirui Gao, Xiaofeng Gao, Paul Weng, and Guihai Chen. Dual sequential prediction models linking sequential recommendation and information dissemination. In *KDD*, pages 447–457. ACM, 2019. 2

[19] Woojeong Jin, Changlin Zhang, Pedro A. Szekely, and Xiang Ren. Recurrent event network for reasoning over temporal knowledge graphs. *CoRR*, abs/1904.05530, 2019. URL `http://arxiv.org/abs/1904.05530`. 2

[20] Jeffrey D. Scargle. An introduction to the theory of point processes, vol. I: elementary theory and methods. *Technometrics*, 46(2):257, 2004. 3

[21] Hongyuan Mei and Jason Eisner. The neural hawkes process: A neurally self-modulating multivariate point process. In *NIPS*, pages 6754–6764, 2017. 3, 14

[22] Shuang Li, Shuai Xiao, Shixiang Zhu, Nan Du, Yao Xie, and Le Song. Learning temporal point processes via reinforcement learning. *Advances in neural information processing systems*, 31, 2018.

[23] Hengguan Huang, Hao Wang, and Brian Mak. Recurrent poisson process unit for speech recognition. In *Proceedings of the AAAI Conference on Artificial Intelligence*, volume 33, pages 6538–6545, 2019. 3

[24] Herbert Jaeger. *Tutorial on training recurrent neural networks, covering BPPT, RTRL, EKF and the" echo state network" approach*, volume 5. GMD-Forschungszentrum Informationstechnik Bonn, 2002. 3

[25] Rakshit Trivedi, Hanjun Dai, Yichen Wang, and Le Song. Know-evolve: Deep temporal reasoning for dynamic knowledge graphs. In *ICML*, volume 70 of *Proceedings of Machine Learning Research*, pages 3462–3471. PMLR, 2017. 3

[26] Weichang Wu, Huanxi Liu, Xiaohu Zhang, Yu Liu, and Hongyuan Zha. Modeling event propagation via graph biased temporal point process. *IEEE Transactions on Neural Networks and Learning Systems*, pages 1–11, 2020.

[27] Eric C. Hall and Rebecca M. Willett. Tracking dynamic point processes on networks. *IEEE Trans. Inf. Theory*, 62(7):4327–4346, 2016. 3

[28] Yuanfu Lu, Xiao Wang, Chuan Shi, Philip S. Yu, and Yanfang Ye. Temporal network embedding with micro- and macro-dynamics. In *CIKM*, pages 469–478. ACM, 2019. 3

[29] Yuan Zuo, Guannan Liu, Hao Lin, Jia Guo, Xiaoqian Hu, and Junjie Wu. Embedding temporal network via neighborhood formation. In *KDD*, pages 2857–2866. ACM, 2018. 3

[30] Jiangxia Cao, Xixun Lin, Xin Cong, Shu Guo, Hengzhu Tang, Tingwen Liu, and Bin Wang. Deep structural point process for learning temporal interaction networks. In *ECML/PKDD*, pages 447–457. Springer, 2021. 3

[31] Oleksandr Shchur, Ali Caner Türkmen, Tim Januschowski, and Stephan Günnemann. Neural temporal point processes: A review. In *IJCAI*, pages 4585–4593. ijcai.org, 2021. 4

[32] E. Çinlar and R. A. Agnew. On the superposition of point processes. *Journal of the Royal Statistical Society: Series B (Methodological)*, 30(3):576–581, 1968. 5

[33] Thomas N. Kipf and Max Welling. Semi-supervised classification with graph convolutional networks. In *ICLR (Poster)*. OpenReview.net, 2017. 6

[34] Kyunghyun Cho, Bart van Merriënboer, Caglar Gulcehre, Dzmitry Bahdanau, Fethi Bougares, Holger Schwenk, and Yoshua Bengio. Learning phrase representations using RNN encoder–decoder for statistical machine translation. In *Proceedings of the 2014 Conference on Empirical Methods in Natural Language Processing (EMNLP)*, pages 1724–1734, Doha, Qatar, October 2014. Association for Computational Linguistics. doi: 10.3115/v1/D14-1179. 6, 15, 16

[35] Anmol Madan, Manuel Cebrian, Sai Moturu, Katayoun Farrahi, et al. Sensing the" health state" of a community. *IEEE Pervasive Computing*, 11(4):36–45, 2011. 6, 14, 15

[36] Alan G Hawkes. Spectra of some self-exciting and mutually exciting point processes. *Biometrika*, 58(1):83–90, 1971. 6, 16

[37] Minjie Wang, Lingfan Yu, Da Zheng, Quan Gan, Yu Gai, Zihao Ye, Mufei Li, Jinjing Zhou, Qi Huang, Chao Ma, Ziyue Huang, Qipeng Guo, Hao Zhang, Haibin Lin, Junbo Zhao, Jinyang Li, Alexander J Smola, and Zheng Zhang. Deep graph library: Towards efficient and scalable deep learning on graphs. *ICLR Workshop on Representation Learning on Graphs and Manifolds*, 2019. 7

[38] Vincent D Blondel, Jean-Loup Guillaume, Renaud Lambiotte, and Etienne Lefebvre. Fast unfolding of communities in large networks. *Journal of statistical mechanics: theory and experiment*, 2008(10):P10008, 2008. 7

[39] Clara Meister and Ryan Cotterell. Language model evaluation beyond perplexity. In *ACL/IJCNLP (1)*, pages 5328–5339. Association for Computational Linguistics, 2021. 7

[40] Shuai Xiao, Mehrdad Farajtabar, Xiaojing Ye, Junchi Yan, Le Song, and Hongyuan Zha. Wasserstein learning of deep generative point process models. *arXiv preprint arXiv:1705.08051*, 2017. 7

[41] David Savage, Qingmai Wang, Xiuzhen Zhang, Pauline Chou, and Xinghuo Yu. Detection of money laundering groups: Supervised learning on small networks. In *AAAI Workshops*, volume WS-17 of *AAAI Technical Report*. AAAI Press, 2017. 9

[42] Ashis Kumar Das, Shiba Mishra, and Saji Saraswathy Gopalan. Predicting covid-19 community mortality risk using machine learning and development of an online prognostic tool. *PeerJ*, 8: e10083, 2020. 9

[43] M Yusuf Özkaya, Ali Pinar, and Ümit V Çatalyürek. Trigger: Temporal interaction graph generator. In *submitted for conference publication*, 2018. 10

[44] Wei Zhang, Xiaogang Wang, Deli Zhao, and Xiaoou Tang. Graph degree linkage: Agglomerative clustering on a directed graph. In *ECCV (1)*, volume 7572 of *Lecture Notes in Computer Science*, pages 428–441. Springer, 2012. 10

[45] Filippo Maria Bianchi, Daniele Grattarola, and Cesare Alippi. Spectral clustering with graph neural networks for graph pooling. In *ICML*, volume 119 of *Proceedings of Machine Learning Research*, pages 874–883. PMLR, 2020. 10

[46] Odd Aalen, Ornulf Borgan, and Hakon Gjessing. *Survival and event history analysis: a process point of view*. Springer Science & Business Media, 2008. 14

[47] Yongqing Wang, Huawei Shen, Shenghua Liu, Jinhua Gao, and Xueqi Cheng. Cascade dynamics modeling with attention-based recurrent neural network. In Carles Sierra, editor, *Proceedings of the Twenty-Sixth International Joint Conference on Artificial Intelligence, IJCAI 2017, Melbourne, Australia, August 19-25, 2017*, pages 2985–2991. ijcai.org, 2017. doi: 10.24963/ijcai.2017/416. 14

[48] Shuai Xiao, Junchi Yan, Xiaokang Yang, Hongyuan Zha, and Stephen M. Chu. Modeling the intensity function of point process via recurrent neural networks. In Satinder P. Singh and Shaul Markovitch, editors, *Proceedings of the Thirty-First AAAI Conference on Artificial Intelligence, February 4-9, 2017, San Francisco, California, USA*, pages 1597–1603. AAAI Press, 2017. 14

[49] Oleksandr Shchur, Ali Caner Türkmen, Tim Januschowski, and Stephan Günnemann. Neural temporal point processes: A review. In *IJCAI*, pages 4585–4593. ijcai.org, 2021. 14

[50] Yichen Wang, Nan Du, Rakshit Trivedi, and Le Song. Coevolutionary latent feature processes for continuous-time user-item interactions. In *NIPS*, pages 4547–4555, 2016. 14

[51] Shuang Li, Shuai Xiao, Shixiang Zhu, Nan Du, Yao Xie, and Le Song. Learning temporal point processes via reinforcement learning. In *NeurIPS*, pages 10804–10814, 2018. 14

[52] Mehrdad Farajtabar, Yichen Wang, Manuel Gomez-Rodriguez, Shuang Li, Hongyuan Zha, and Le Song. Coevolve: A joint point process model for information diffusion and network evolution. *The Journal of Machine Learning Research*, 18(1):1305–1353, 2017. 14

[53] Amanda Andrei, Alison Dingwall, Theresa Dillon, and Jennifer Mathieu. Developing a tagalog linguistic inquiry and word count (LIWC) 'disaster' dictionary for understanding mixed language social media: A work-in-progress paper. In *LaTeCH@EACL*, pages 91–94. The Association for Computer Linguistics, 2014. 15

[54] Ilya Sutskever, Oriol Vinyals, and Quoc V Le. Sequence to sequence learning with neural networks. In Z. Ghahramani, M. Welling, C. Cortes, N. Lawrence, and K. Q. Weinberger, editors, *Advances in Neural Information Processing Systems*, volume 27. Curran Associates, Inc., 2014. 16

[55] Ashish Vaswani, Noam Shazeer, Niki Parmar, Jakob Uszkoreit, Llion Jones, Aidan N. Gomez, Lukasz Kaiser, and Illia Polosukhin. Attention is all you need. In *NIPS*, pages 5998–6008, 2017. 17

A The Illustration Figure of Community Event Forecasting Task

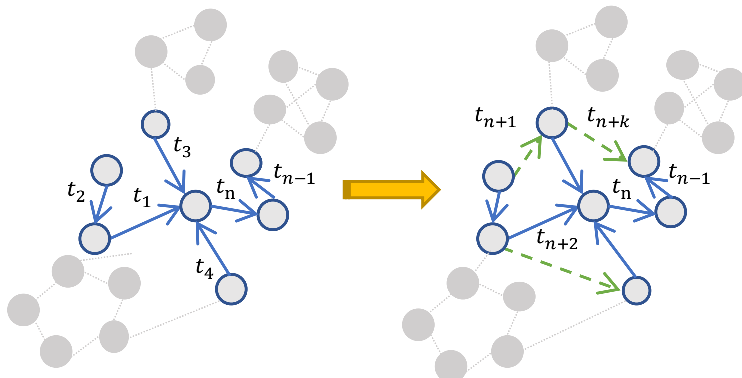

Figure 5: Community event forecasting on a CTDG: Given a community (nodes and edges with blue strokes) in a historical CTDG, predict where and when the next interaction event (green arrows) will happen. This process can be repeated to forecast to distant future.

B Preliminaries of Temporal Point Process

A TPP is mostly characterized by a conditional intensity function $\lambda(t)$, from which it computes the conditional probability of an event occurring between t and $t + dt$ given the history $\{t_i : t_i < t\}$ as $\lambda(t)dt$. According to [46], the log conditional probability density of an event occurring at time t can be formulated as

$$f(t) = \log \lambda(t) - \int_{t_n}^{t} \lambda(\tau) d\tau \tag{14}$$

Additionally, a marked temporal point process (MTPP) associates each event with a *marker* y_i which is often regarded as the *type* of the event. MTPP thus not only models when an event would occur, but also models what type of event it is. Event forecasting over CTDGs can also be modeled as a MTPP if treating the event's incident node pair as its marker. The conditional intensity of the entire MTPP can be modeled as a sum of conditional intensities of each individual marker: $\lambda = \sum_m \lambda_m$. This allows it to first make the prediction of event time, and then predict the marker conditioned on time via sampling from a categorical distribution: $m \sim \text{Categorical}(\lambda_m)$. This avoids modeling time and marker jointly. Such idea has been widely used in follow-up works such as Recurrent Marked Temporal Point Process (RMTPP) [13]. RMTPP parametrizes the conditional intensity and the marker distribution with a recurrent neural network (RNN). RMTPP's variants include CyanRNN [47] and ARTPP [48].

We also demonstrate several other relevant works and applications related to TPPs [49]. CoEvolving [50], a variant model of MTPP, uses Hawkes processes to model the user-item interaction, respectively. NeuralHakwes [21] relaxes the positive influence assumption of the Hawkes process by introducing a self-modulating model. DeepTPP [51] models the event generation problem as a stochastic policy and applied inverse reinforcement learning to efficiently learn the TPP. [52] models link and retweet generation on a social network with a TPP, and also provides a simulation algorithm that generates from the TPP model. It is very similar to our task except that it is focused on a specific social network setting, and the authors did not quantitatively evaluate the quality of the simulation model.

C Datasets

In this section, we test the performance and efficiency of the proposed method against multiple baselines on four public real-world temporal graph datasets: Wikipedia, MOOC [10], GitHub [14], and SocialEvo [35]. Table 2 shows summary statistics of the datasets used in our experiments. A detailed description is put in the below.

Table 2: Statistics of the datasets used in our experiments.

Level	Statistics	Wikipedia	MOOC	Github	SocialEvo
Graph level	Edges	157,474	411,749	20,726	62,009
	Nodes	9,227	7,145	282	83
	Aver. Event	34	115	147	1,310
	Aver. Unique Neighbors	1.98	24.98	14.65	9.02
	Edge Feat. Dim.	172	4	10	10
	Unique Edges in Graph	5.99%	19.95%	10.27%	0.62%
	Is Bipartite	True	True	False	False
	Timespan	31days	30days	1years	74days
	Edges/hour	211.66	576.30	2.36	7.79
	Data Spilt	70%-15%-15% by timestamp order			
Community level	Communities	142	25	17	10
	Max Nodes	396	990	46	18
	Aver. Nodes	50.27	264.96	15.94	7.7
	Max Edges	4799	11686	3221	12199
	Aver. Edges	778.28	2560.00	534.71	3420.90
	Min Edges	77	16	34	863
	Max Edges/hour	6.47	33.33	0.36	1.99
	Aver. Edges/hour	1.11	5.36	0.06	0.56
	Min Edges/hour	0.14	0.34	0.01	0.15

Wikipedia [10] dataset is widely used in temporal-graph-based recommendation systems. It is a bipartite graph consisting of user nodes, page nodes and edit events as interactions. We convert the text of each editing into a edge feature vector representing their LIWC categories [53].

MOOC [10] dataset, collected from a Chinese MOOC learning platform XuetangX, consists of students' actions on MOOC courses, e.g., viewing a video, submitting an answer, etc.

Github [14] dataset is a social network built from GitHub user activities, where all nodes are real GitHub users and interactions represent user actions to the other's repository such as Watch, Fork, etc. Note that we do not use the interaction types as we follow the same setting as [14].

SocialEvo [14, 35] dataset is a small social network collected by MIT Human Dynamics Lab.

Since the public dataset SocialEvo and Github have no edge feature, we generate a 10-dimensional edge feature using following attributes, including the current degrees of the two incident nodes of an edge, and the time differences between current timestamp and the last updated timestamps of the two incident nodes. "Percentage of unique edges" represents the likelihood that new events already happened, and "Average unique neighbors" measures the likelihood that entities on the graph will seek out connections with other entities that have never interacted with them. Note that the time differences are described in the numbers of days, hours, minutes and seconds, respectively.

D Baselines

Table 3: Comparison of model capabilities. Note that the usage of RNN prevents a model from parallel training as is mentioned in Section 2.3. *Requires non-trivial adaptation.

Taxnomy	GNN+TPP		RNN+TPP	GNN	TPP	
Methods	CEP3	DyRep	RMTPP	TGAT	Poisson	Hawkes
Predicts Link (u,v)	√	√	√	√	√	√
Predicts Continuous Time t	√	√	√		√	√
Jointly Predicts Event (u,v,t)	√	√*	√		√	√
Explicitly Models Topological Dependency	√	√		√		
Complexity of Node Prediction	$O(\|V\|)$	$O(\|V\|^2)$	$O(\|V\|^2)$	$O(\|V\|^2)$	$O(\|V\|^2)$	$O(\|V\|^2)$
Parallel Training	√			√	√	
Captures Sequential Info with	Attention	RNN+Attention	RNN	Attention	Poisson Process	Hawkes Process

In addition to **CEP3**, **CEP3 w RNN**, **CEP3 w/o HRCHY**and **CEP3 w/o AR** mentioned in Section 3, we compare against the following baselines: a Seq2seq model with a **GRU** [34], a Poisson Process

(**TPP-Poisson**), a Hawkes Process (**TPP-Hawkes**) [36], **RMTPP** [13] and its variant with the same two-level hierarchical factorization as in Eq. 8 and 9 (**RMTPP w HRCHY**), an adaptation of DyRep [14] and an auto-regressive variant (named **DyRep** and **DyRep w AR**). Notably, RMTPP and its variants are SOTA models for MTPPs in general, and DyRep is SOTA in temporal link prediction and time prediction on CTDG. Since our task is new, we made adaptations to the baselines above, with details of each baseline is as follows:

Time series Methods: For baseline model of sequential prediction, we build an RNN model, Gated Recurrent Unit (GRU). Each source and destination cell has a hidden state, the output of the model will be predicted time mean and variance as well as probability for each class to interact, the time will be formulated as Gaussian distribution and source and destination node will be formulated as categorical distribution. This formulation forces GRU predicting timestamp of upcoming events only depending on the hidden state in RNN, whereas other baselines adapt TPP function as a stochastic probability process, obtaining a better modeling capability. We use a **GRU** [34] as a simple baseline without using TPP to model time distribution, treating event forecasting on CTDG as a sequential modeling task. It takes in the event sequence and outputs the next K event in a Seq2seq fashion [54]. The loss term for time prediction is mean squared error and the loss term for source and destination prediction is the negative log likelihood. This formulation forces GRU to predict the timestamp of upcoming events only depending on the hidden state in RNN, whereas other baselines adapt TPP for better modeling capabilities.

Temporal Point Process Methods: Following the benchmark setting of [13], we compared our model against other traditional TPP models and deep TPP models.

- **TPP-Poisson**: We assume that the events occurring at each node pair (u, v) follows a Poisson Process with a constant intensity value $\lambda_{u,v}$, which are learnt from data via Maximum Likelihood Estimation (MLE).
- **TPP-Hawkes** [36]: We assume that the events occurring at each node pair (u, v) follows a Hawkes Process with a base intensity value $\mu_{u,v}$ and an excite parameter $\alpha_{u,v}$, which are learnt from data via MLE.
- **RMTPP** [13]: We directly consider each source and destination node pair as a unique marker. We note that this formulation will exhaust memory and time on graphs with more than a few thousand nodes, since RMTPP will assign a learnable embedding for each node pair, resulting in $O(|V|^2)$ (Here V is total number of nodes in the entire CTDG) parameters which is too expensive to update.
- **RMTPP w HRCHY**: We consider a variant of RMTPP where we replace the source-destination node prediction with our hierarchical formulation: we first select the source node, then condition on the source node we select the destination node. The latter formulation can also serves as an ablation study to demonstrate the usage of considering the graph structure.
- **DyRep** [14]: DyRep is a popular work that combine the temporal point process with graph learning techniques to model both temporal and spatial dependencies. Since the original DyRep formulation only handles temporal link prediction and time prediction, but not autoregressive forecasting, we compute an intensity value $\lambda_{u,v}$ with DyRep for each node pair and assumed a Poisson Process afterwards.
- **DyRep w AR**: We made a trivial adaptation to the original formulation of DyRep by updating the source and destination node involved once a new edge is added to the graph. The update function is identical to DyRep updating function during embedding. This benchmark is designed to demonstrate that the propagation from newly forecast event to local neighborhood is necessary in getting better performance.

We also crave our proposed model for having the ability to implement minibatch training. As described in the beginning of Section 3, our CEP3 achieves large-scale and parallelized training by utilizing Hierarchical TPP and GNN based updating module, respectively. A summary of the mentioned baselines is shown in Table 3, the proposed model CEP3 satisfies all the desirable properties.

E Configuration

We provide the details of our network architecture, the hyper-parameters and the selected community detection method for better reproducibility. Table 4 summarizes other key parameters in our model.

Table 4: Configurations for our CEP3 and all baselines.

Name	Value
Hidden Dim in Encoder	100
Hidden Dim in Forecaster	50
Hidden Dim in Time Encoding	100
Layers in MLPs	2
K-hops	2
Sampled neighbors/Hop	15
Learning rate	0.0001
Optimizer	Adam
# of attn head	4
Recurrent Module	GRU
Epochs	100
Forecasting Window	200 Steps
Community Detection Method	Louvain

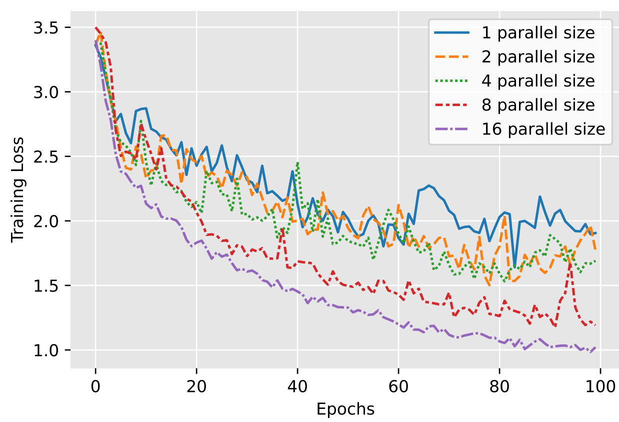

Figure 6: Training loss curve with different parallel sizes.

For all the experiments we train our model and benchmark models on Intel(R) Xeon(R) Platinum 8375C CPU @ 2.90GHz.

F Parallel Training

Inspired by the Transformer [55] models in NLP, we believe it is essential to use a pure attention-based model in temporal graph encoders. This is because using a pure attention-based GNN as an encoder enables us to train multiple time windows in minibatches as described in Section 3.1, whereas the model such as Dyrep and RMTPP cannot utilize parallel training due to their RNN structures. This property allows our model to benefit from mini-batch training such as gradient stabilization and faster convergence. Fig. 6 shows our experiment result on the Wikipedia dataset with different numbers of parallel processes, suggests that using parallel training can increase the speed significantly without losing accuracy.